**ACTS-P00321**

# LOCAL HEAT TRANSFER CHARACTERISTICS AND VORTEX STRUCTURES OF VISCOELASTIC FLUIDS IN SERPENTINE CHANNELS

**K. Tatsumi †*, N. Shinotsuka, R. Kimura, R. Kuriyama and K. Nakabe**

Kyoto University, Kyotodaigaku-katsura, Nishikyo-ku, Kyoto 615-8540, Japan

†*Presenting and Corresponding Author: tatsumi@me.kyoto-u.ac.jp

## ABSTRACT

In this study, we focus on the flow instability and the generation of the strong unsteady flow in serpentine channels under very low Reynolds number conditions of *Re*~1. The local heat transfer, pressure loss and flow characteristics of the viscoelastic fluid in the transition and developed flows through a serpentine channel were measured and described. Water solution of polyacrylamide with sucrose was used as viscoelastic fluid. The results showed that the flow becomes unsteady and longitudinal vortices-like secondary flows were generated due to the normal stress differences produced by the viscoelasticity of the fluid located near the top and bottom walls. This enhanced the heat transfer performance markedly. The vortex structures changed depending on the streamwise position and Weissenberg number *Wi* showing three transition stages: a pair of moderate vortices, a single vortex with a drift of main flow toward the wall, and a pair of strong vortices. These vortices affected the local heat transfer characteristics at the top/bottom walls and sidewalls, streamwise distributions, and their unsteady behavior. We showed that these behaviors and characteristics could be correlated by the combination of *Wi* and *Re*.

**KEYWORDS:** Viscoelastic fluid, Serpentine channel, Heat transfer, Convection, Low Reynolds number flow, Unsteady flow, Vortex structure

## 1. INTRODUCTION

Viscoelastic fluid produces interesting and effective flow structures and features in various channels and conditions. One of these effects is the increase of the flow instability which induces the generation of unsteady flows under low Reynolds number conditions. The viscoelasticity can also generate additional stresses due to the normal stress differences which leads to the generation of secondary flows. Such unsteady flow and vortices can enhance the fluid mixing and heat transfer at the channel walls [1, 2]. Intensive work has been made to study these effects with various channel shapes and under wide range of flow conditions [3-5]. In our pervious works, we have been focusing on the flow and heat transfer characteristics of viscoelastic fluid in serpentine channel (schematic is shown in Fig. 1). We have confirmed that the average heat transfer performance can be enhanced due to the generation of longitudinal vortex like secondary flows and its unsteady behavior [6, 7].

In this study, measurements of flow visualization and the local heat transfer coefficient are carried out. The developing and developed regions of the flow and heat transfer were studied by measuring the heat transfer coefficient at different streamwise positions and flow rates. Further, the viscoelastic properties of the fluid were changed to discuss the appropriate dimensionless number to correlated the heat transfer and pressure loss characteristics. From these results, the relationship between the flow structure and heat transfer characteristics are discussed to understand the mechanism of heat transfer enhancement.

## 2. EXPERIMENTAL METHODS AND CONDITIONS

Figure 1 shows the experimental apparatus and the serpentine channel of the present study. The serpentine channel had a square cross section 5 mm on a side, and consisted of semicircle parts connected periodically in the streamwise direction. The number of the curve units, *N*, was 30. Constant heat flux conditions were applied to the

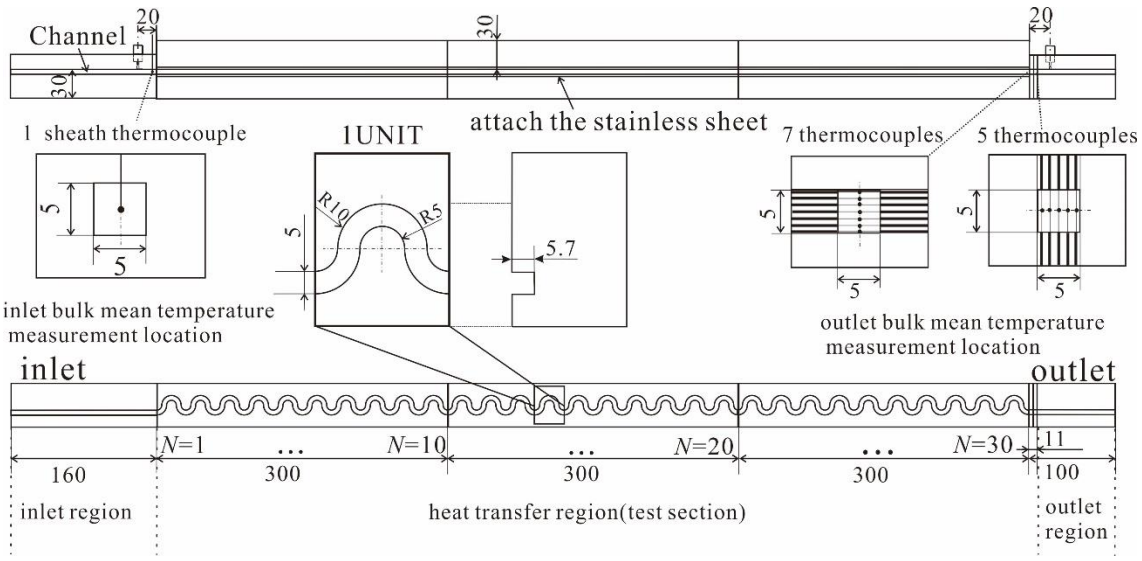


**Fig. 1** The channel and test section of the heat transfer and flow visualization measurements.

channel walls. Two test sections, one with the top and bottom walls heated, and the other with sidewalls heated were used to measure the heat transfer coefficient of each wall. Stainless steel sheets were attached to the wall to apply constant heat flux while the local wall temperature was measured to obtain the heat transfer coefficients.

The unheated walls were made transparent to perform the flow visualization through the walls simultaneously with the heat transfer measurement. The streak lines were visualized by recording the image of the ink dye supplied to the flow through a needle set in the upstream region of the channel. The flow pressure loss was measured by two pressure gauges installed to the inlet and outlet of the test section, respectively.

Aqueous solution of 500ppm polyacrylamide (PAAm, MW: $1.8\times10^7$) was used as viscoelastic fluids. To stable the fluid properties, 1wt% NaCl was added. Sucrose was mixed with the concentration of 57.0, 60.0 and 64.4wt% to increase the viscosity and relaxation time of the fluid. Aqueous solution of 64.4wt% sucrose only (Newtonian fluids) was also measured for comparison. The fluid viscosity and relaxation time were measured by a rheometer in advance of each experiment. The flow rate was changed and the related flow conditions ranged as follows based on the dimensionless number: Reynolds number, $Re$=0.2-5.8, Graetz number, $Gz$=3-40, Weissenberg number, $Wi$=8-137, and Dean number, $N_D$=0.1-3.5.

## 3. RESULTS AND DISCUSSION

Figure 2 shows the Nusselt number $Nu_m$ distributions in relation to $Re$ and $Wi$. $Nu_m$ averaged in the streamwise region of $N$=21-30 is shown in the figure. At $Re$<0.3 or $Wi$<20, $Nu_m$ of PAAm cases matches with the solid line showing that the flow structure is similar to that of the steady state laminar flow of Newtonian fluid. As $Re$ increases $Nu_m$ increases. However, the $Re$ at which $Nu_m$ starts to increases in the cases of PAAm(54), PAAm(60) and PAAm(67) do not correspond with each other. On the other hand, a good correlation among these three distributions are observed with $Wi$ shown in Fig. 2(b). This indicates that the heat transfer characteristics are attributed more to the vortices generated by the normal stress differences of the viscoelastic fluid than the fluid dynamic instability characteristic.

Figure 3 shows $Nu_m$ in the cases when the top-bottom walls and sidewalls were heated. $Nu$ shown here are the averaged values of the sections dividing the channel into three with each part composed of 1-10th, 11-20th and 21-30th curve units. The $Re$ in which $Nu_m$ starts to increase are of a same value in the three regions. This shows that the flow becomes unsteady and vortex is generated nearly at the same time through the channel. However, the distribution does not increase monotonically and shows a characteristic pattern in relation to the streamwise position and $Wi$ particularly in the sidewall heated case. Taking the visualization results into account, the heat transfer characteristics can be roughly divided into several regions which are shown in Fig. 3 (b) as (A), (B), (C) and (D).

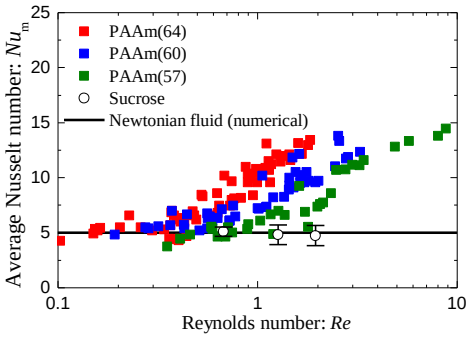


(a) $Nu_m$ vs $Re$

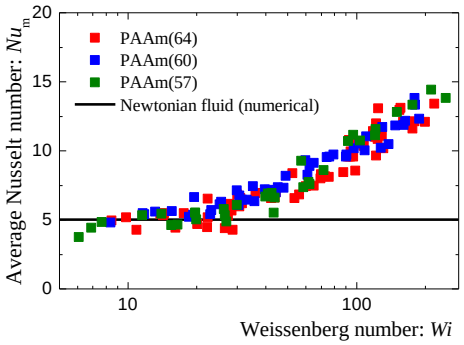


(b) $Nu_m$ vs $Wi$

**Fig. 2** Average Nusselt number $Nu_m$ in relation to Reynolds number $Re$ and Weissenberg number $Wi$. $Nu_m$ is averaged in the region of $N$=21-30, and PAAm(57), PAAm(60) and PAAm(64) are the cases of PAAm soluton with sucrose 57.0, 60.0 and 64.4wt% concentrations, respectively.

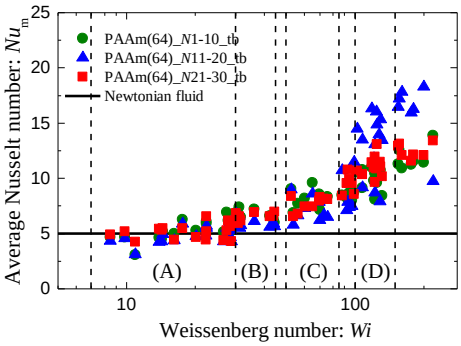


(a) $Wi$ vs $Nu_m$ (top-bottom walls)

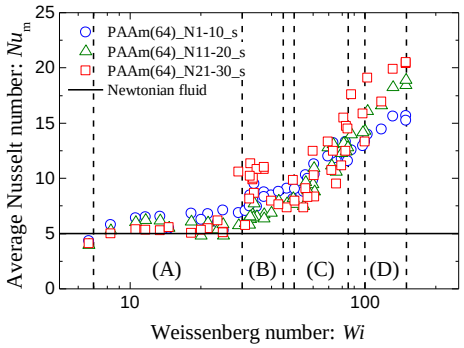


(b) $Wi$ vs $Nu_m$ (sidewalls)

**Fig. 3** Locally averaged Nusselt number $Nu_m$ distributions of top-bottom and sidewalls in the case of PAAm(64). $Nu_m$ is averaged in three regions, $N$=1-10, 11-20 and 21-30, respectively.

Figure 4 shows the local Nusselt number $Nu_x$ distributions of the top-bottom walls and sidewalls averaged in several $Wi$ regions. These regions roughly correspond to those shown in Fig. 3 (b). Figure 5 shows the time distributions of $Nu_x$ at the top-bottom walls of $N$=16, and the flow visualization performed simultaneously at the same location. The period (b)-(f) shown by the dash lines in Fig. 5 (a) corresponds to those of Figs. 5 (b)-(f).

As shown in Fig. 4, $Nu_x$ begins to increase from the downstream showing that the secondary flow generation and unsteady flow starts from the downstream side. Larger $Nu_x$ is observed in the sidewall compared to the top-bottom walls. This is due to the generation of a pair of longitudinal vortices like secondary flow which carries the low temperature fluid located at the channel center toward the outer wall of the curvature and increases $Nu$ there. This can be confirmed by comparing the $Nu_x$ and flow structure shown in Fig 5 particularly in the cases of (b) and (e).

The error bar shown in Fig. (4) increases with $Wi$. This error bar is the deviation of the instantaneous $Nu_x$ from the averaged one. Therefore, it presents the fluctuation of the heat transfer coefficient and the flow and not the measurement error. As shown in Fig. 5, the direction of the pair of vortices changes related to the height position of the flow core region: as the region of high velocity moves in the height direction, the normal stress changes its amplitude in the region adjacent to the top and bottom walls leading to the change of the vortices direction. The instantaneous $Nu_x$ changes and fluctuates over time due to this change of the flow structure.

Thus we can explain the heat transfer and flow characteristics of regions (A)-(D) as follows.

In region (A), the flow structure is nearly the same with the Newtonian fluid flow. In region (B), as mention in above, secondary flow is observed and the flow becomes unsteady. $Nu_m$ of the sidewalls increases while $Nu_m$ slightly decreases in the case of top-bottom walls heated. Further, a noticeable peak appears in the N21-30 region of the sidewall heated case.

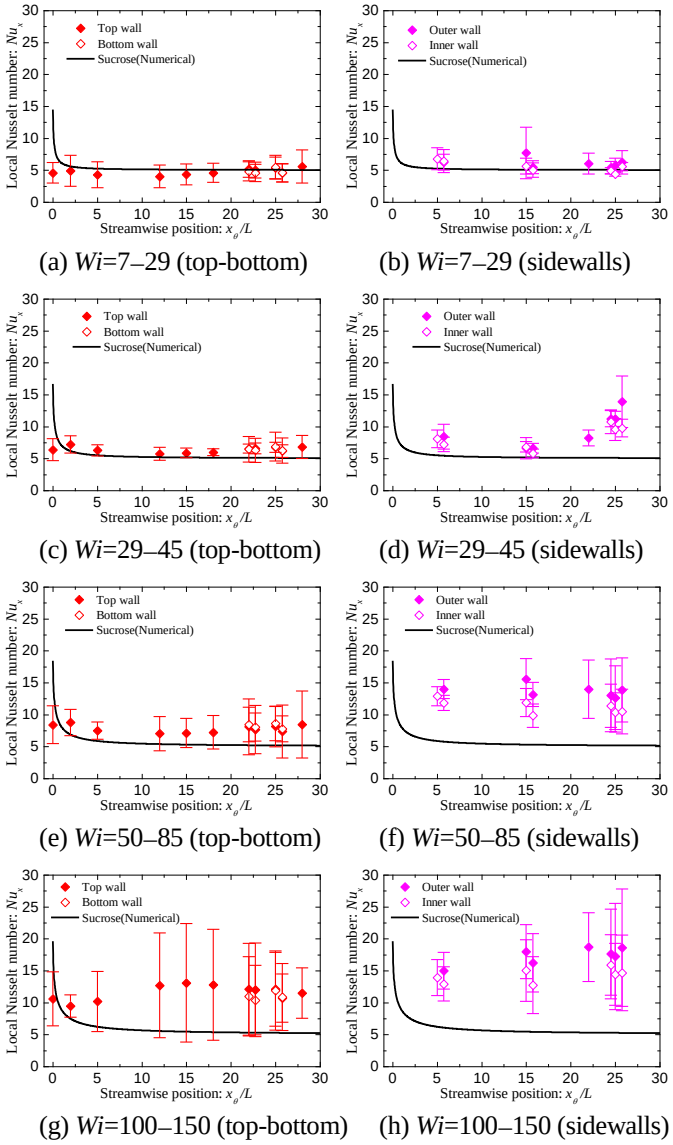


**Fig. 4** Streamwise local Nusselt number distributions at the top-bottom walls and sidewalls in the *Wi* four regions (A)-(D) shown in Fig. 3.

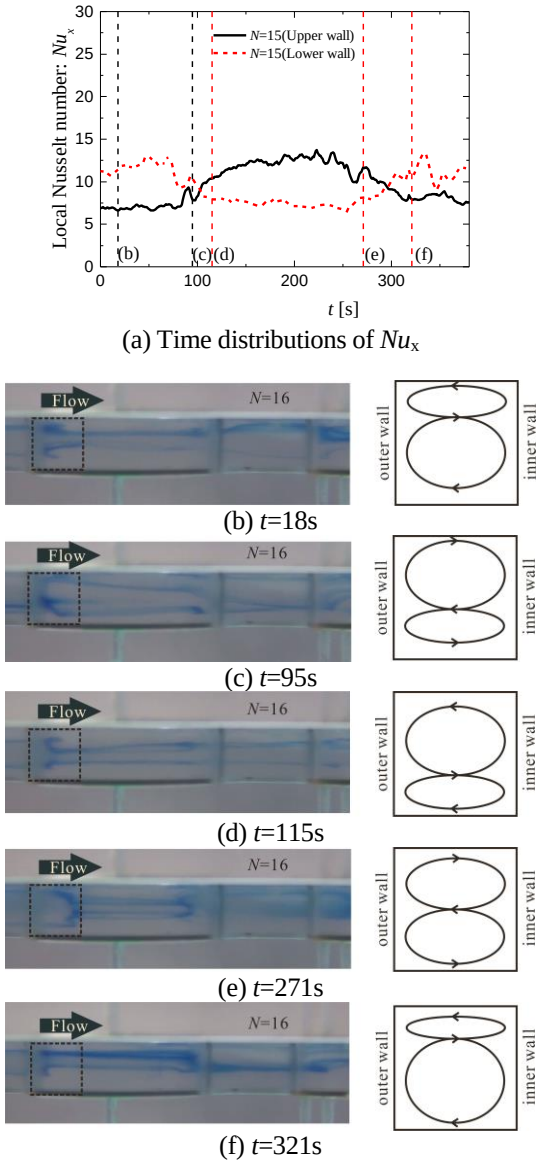


**Fig. 5** Simultaneous measurement of $Nu_x$ and visualization. (a) Time distributions of $Nu_x$ and (b) side views of the streaklines both measured at $N$=16.

In this *Wi* region, a pair of longitudinal vortices like secondary flows are generated in the channel. This secondary flow generation is attributed to the normal stress difference of the viscoelastic fluid, and convects the fluid located at the channel center toward the outer wall while the fluid located adjacent to the outer wall is driven toward the top-bottom walls. Therefore, the $Nu_m$ at the sidewalls is enhanced while the $Nu_m$ at the top-bottom walls decrease. These secondary flow is fully developed at the downstream side of the channel, and, thus, a marked increase of $Nu_m$ is observed in Fig. 3 (b).

In region (C), these pair of vortices develop to a single vortex. The vortices in this region becomes unstable, and one of the two vortices increases its size and occupy a large portion of the cross section. Further, the main flow is located near the center of this larger secondary flow, and drifts toward one side of the top-bottom walls increasing the $Nu_m$ there. As mentioned above, the direction of the vortices changes depending on the location of the flow core.

In region (D), a symmetric pair of vortices appears again from the downstream of the channel. As *Wi* increases, the normal stress described in the discussion of region (B) increases. This makes the pair of vortices become more stable, and thus the single vortex like secondary flow and the drift of the main flow in the height direction decay. Thus, the phenomena observed in region (C) moves upstream to the N11-20 region, the region at which we can find the fluctuation of $Nu_x$ at the top-bottom walls increasing. On the other hand, in the N21-30 region, the sidewall heat transfer increases markedly and the fluctuation decreases compared to those of top-bottom walls. The fluctuation at the sidewalls, however, still shows a large value due to the change of the direction of the pair of vortices.

## 4. CONCLUSIONS

Heat transfer coefficient, flow visualization and pressure loss measurement were conducted for viscoelastic fluid in serpentine channel under low Reynolds number conditions of *Re*~1. The average Nusselt number *Nu* increased as the *Re* and Weissenberg number *Wi* increased showing a three times higher heat transfer performance compared to Newtonian fluid. A better correlation was observed between the *Wi* number and *Nu* number indicating that the vortices generation and unsteady flow which increase the *Nu* was mainly attributed to the normal stress of the viscoelastic fluid. The local *Nu* and flow structure varied in the streamwise location, top-bottom and sidewall, and *Wi* conditions. This was mainly due to the difference of vortex structure: a pair of longitudinal vortices, a single vortex with the position of the core region – high flow velocity region – changing in the height direction, and a pair of strong longitudinal vortices changing their rotational directions.

## ACKNOWLEDGMENT

This work was partially supported by JSPS KAKENHI Grant Number 24360080 and 25630066.

## NOMENCLATURE

| | | | | | |
|---|---|---|---|---|---|
| $D$ | hydraulic diameter | (m) | Re | Reynolds number, $\rho U_m D/\mu_0$ | ( - ) |
| $U_m$ | mean flow velocity | (m/s) | Wi | Weissenberg number, $4U_m\lambda/D$ | ( - ) |
| $\lambda$ | relaxation time | (s) | $\mu_0$ | zero-shear-rate viscosity | (Pa s) |
| $\rho$ | fluid density | (kg/m$^3$) | | | |

## REFERENCE

[1] J. P. Hartnett and M. Kostic, Heat Transfer of a Viscoelastic Fluid in Laminar Flow through a Rectangular Channel, Int. J. Heat and Mass Transfer. 28 (1985) 1147-1155.
[2] X. Chunbo and J.P. Hartnett, Influence of Rheology on Laminar Heat Transfer to Viscoelastic Fluids in a Rectangular Channel, Ind. Eng. Chem. Res. 31 (1992) 727-732.
[3] A. Groisman and V. Steinberg, Efficient Mixing at Low Reynolds Numbers Using Polymer Additives, Nature. 410 (2001) 905-908.
[4] S. Tamano, M. Itoh, M. Sasakawa and K. Yokota, PIV Measurement of Secondary Flow in Curvilinear Pipe Flow of Polymer Solution, Transactions of the JSME. Ser. B. 75 (2009) 2115-2121.
[5] J. Zilz, R. J. Poole, M. A. Alves, D. Bartolo, B. Levache and A. Lindner, Geometric Scaling of a Purely Elastic Flow Instability in Serpentine Channels, J. Fluid Mech. 712 (2012) 203-218.
[6] K. Tatsumi, W. Nagasaka, O. Nakajima, C. L. Heong, and K. Nakabe, Flow and Heat Transfer Characteristics of Viscoelastic Fluid Flow in a Serpentine Channel, Transactions of the JSME. Ser. B. 79 (2013), 93-103.
[7] K. Tatsumi, W. Nagasaka, T. Matsuo and K. Nakabe, A Numerical and Experimental Study on Flow and Heat Transfer Characteristics of Viscoelastic Fluid Flow in a Serpentine Channel, Fifteenth International Heat Transfer Conference, IHTC15. (2014) 9615.